

Refractive index in warm and hot dense matterGérald Faussurier,^{*} Christophe Blancard, and Phillipe Cossé*CEA, DAM, DIF, F-91297 Arpajon, France*

(Received 9 December 2014; published 12 May 2015)

A method to estimate the index of refraction in warm and hot dense matter is proposed. This method combines the Kubo-Greenwood approach, Maxwell equations, and existing codes that calculate photoabsorption and photoemission coefficients in warm and hot dense plasmas. An effective electrical conductivity is calculated from existing opacity codes from which the index of refraction is derived. Illustrations are shown on specific examples.

DOI: [10.1103/PhysRevE.91.053102](https://doi.org/10.1103/PhysRevE.91.053102)

PACS number(s): 52.25.Fi, 52.25.Mq, 52.25.Os

I. INTRODUCTION

The theoretical knowledge of plasma dielectric properties can be very useful to characterize such ionized media. For example, the electron density of a plasma can be evaluated by analyzing optical interferograms of a monochromatic photon beam passing through the considered media. Assuming that the index of refraction of a homogenous plasma is only due to free electrons, the electron density is directly proportional to the number of fringe shifts measured on the interferogram. In such approximation, the index of refraction is lower than unity. Recent interferometry experiments [1,2], involving soft x-ray lasers to probe few ionized low- and mid-Z diluted plasmas, have shown anomalous dispersion phenomena, i.e., observed fringe shifts bend in opposite direction than was expected if the index of refraction is simply given by free electrons. Detailed analysis have shown that bound electron contribution (resonant structures and absorption edge) can dominate the index of refraction resulting in values greater than one. With the development of x-ray-free electron lasers (XFEL), high-density plasmas could be probed. A precise knowledge of plasma dielectric properties in the short wavelength range will then be needed to analyze the interferograms [3].

Various works have been published concerning the optical properties of warm and hot dense matter starting from first principles. Among them, one can distinguish those based on the Kubo-Greenwood approach [4,5] using either quantum molecular dynamics simulations [6–9] or average-atom models [10–13]. The central quantity of interest is the real part of the electronic dynamical electrical conductivity, from which various optical quantities can be obtained using classical Maxwell equations [14–16]. The main advantage of these approaches is the powerful theoretical background from which things are derived. Other works exist concerning the treatment of the free-free component [17–20] or the implementation of bound electrons [21–23] that are crucial to understand some plasma interferometry experiments [1,2,23–25].

If the problem is rather complex and progresses are noticeable, it is not always clear how the different approaches published in the literature are connected, what are their internal degree of consistency and domain of validity, or how they can be improved. Indeed, taking into account the refractive index of the medium is far from being anecdotal [7,26–32], and it raises

many questions concerning the treatment of electrodynamics in dense matter [33].

In this paper, we show how the calculation of the electronic dynamical electrical conductivity in the framework of the Kubo-Greenwood approach using the average-atom model [10–12] is related to the calculation of the photoabsorption and photoemission coefficients [34] in dense plasmas [35], which are assumed to be in local thermodynamical equilibrium (LTE). A method is proposed to estimate the index of refraction in warm and hot dense matter from existing opacity codes that could be useful to interpret XFEL-heating and XUV-probe experiments performed on XFEL setups. Numerical applications are presented and discussed. The last part is the conclusion.

II. THEORY

From the linear response theory in the framework of the nonrelativistic average-atom model, Johnson *et al.* [10] derived bound-bound, bound-free, and free-free expressions for the electronic frequency-dependent electrical conductivity. The described theory is based on the Kubo-Greenwood approach. Note that the changes in the potential due to the perturbing field are neglected, as stated by the authors. No ionic structure treatment is considered. We keep these approximations that should be questioned in future works. In particular, since the average-atom model is a self-consistent field approach, it is not clear to what extent freezing the potential in which one-electron wavefunctions are calculated is legitimate or not. We put aside this question for the moment, neglect the ionic environment, and take as they are the formulas for the three components established by Johnson *et al.* [10]. In this work, since the words electrical conductivity refer to the electronic electrical conductivity, the word electronic will be understood as such when referring to the electrical conductivity.

These formulas are written in terms of the reduced matrix elements of the velocity operator. We first transform them in terms of the reduced matrix elements of the radial operator [34]. Written under this form, we are going to consider successively the free-free, the bound-bound, and the bound-free parts. Note that some care is required concerning the free-free radial matrix-element [28,36–39]. Its explicit calculation in hot dense matter can be a difficult numerical exercise, even if this matrix element is written under the acceleration form [34,39].

^{*}gerald.faussurier@cea.fr

A. Free-free component in the one-electron approximation

Let us start with the free-free component $\sigma_{\text{ff}}(\omega)$ of the real part of the frequency-dependent electrical conductivity [10,34],

$$\sigma_{\text{ff}}(\omega) = \frac{2\pi\omega e^2}{3\Omega} \int_0^\infty d\varepsilon [f(\varepsilon) - f(\varepsilon + \hbar\omega)] \times \sum_{\ell, \ell' = \ell \pm 1} \ell_{>} \left[\int_0^\infty dr P_{\varepsilon, \ell}(r) r P_{\varepsilon + \hbar\omega, \ell'}(r) \right]^2, \quad (1)$$

where ω is the angular frequency, e the elementary charge, \hbar the reduced Planck constant, and Ω the atomic volume related to the Wigner-Seitz radius a_{WS} by the formula $\Omega = 4\pi a_{\text{WS}}^3/3$. One has also $\Omega = 1/N_i$, where N_i is the ionic density. ℓ is the orbital quantum number, and the one-electron radial parts of the free wavefunctions are normalized such that [10]

$$\int_0^\infty dr P_{\varepsilon, \ell}(r) P_{\varepsilon', \ell'}(r) = \delta(\varepsilon - \varepsilon'), \quad (2)$$

where ε is the incident-electron energy and

$$f(\varepsilon) = \frac{1}{1 + e^{\beta\varepsilon - \eta}} \quad (3)$$

is the Fermi-Dirac distribution function. Here, $\beta = 1/k_B T$, where k_B is the Boltzmann constant and T the temperature. η is the dimensionless chemical potential related to the chemical potential μ by $\eta = \beta\mu$. The factor 2 in Eq. (1) accounts for the electron spin. Moreover, $\ell_{>}$ is the maximum of the two orbital quantum numbers of interest, here ℓ and ℓ' . One can check that $\sigma_{\text{ff}}(\omega)$ in Eq. (1) has the proper dimensions.

Let us simplify it using the Kramers approximation [34]. To do this, we consider the nonrelativistic expression of the bremsstrahlung cross-section of an electron in a centrally symmetric field [Eq. (9.241), p. 247 of Ref. [34]], and compare it to the Kramers expression of the bremsstrahlung cross-section of an electron in a Coulomb field [Eq. (9.272), p. 257 of Ref. [34]]. The bremsstrahlung cross-section of an electron in a centrally symmetric field reads

$$\frac{d\sigma_{\varepsilon'; \varepsilon \hbar\omega}}{d\omega} = \frac{8\pi^2 \omega^3 e^2 \hbar}{3 c^3 q^2} \sum_{\ell, \ell' = \ell \pm 1} \ell_{>} \times \left[\int_0^{+\infty} P_{\varepsilon, \ell}(r) r P_{\varepsilon + \hbar\omega, \ell'}(r) dr \right]^2, \quad (4)$$

where $\varepsilon' = (\hbar q)^2/2m_e$, $\varepsilon' = \varepsilon + \hbar\omega$, and c is the speed of light, whereas the Kramers expression of the bremsstrahlung cross-section of an electron in a Coulomb field reads

$$\frac{d\sigma_K}{d\omega} = \frac{16\pi}{3\sqrt{3}} \frac{\bar{Z}^2 e^6}{c^3 \hbar^3 q^2} \frac{1}{\omega}, \quad (5)$$

where \bar{Z} is the effective nuclear charge. If the centrally symmetric field is taken to be a Coulomb field, one can compare Eqs. (4) and (5). If we do this, we find that

$$\sum_{\ell, \ell' = \ell \pm 1} \ell_{>} \left[\int_0^\infty dr P_{\varepsilon, \ell}(r) r P_{\varepsilon + \hbar\omega, \ell'}(r) \right]^2 \approx \frac{2}{\pi\sqrt{3}} \frac{\bar{Z}^2 e^4}{(\hbar\omega)^4}. \quad (6)$$

Note that the result depends only on the energy difference $\hbar\omega$. This kind of approach is usually encountered in opacity calculations [34]. If we inject Eq. (6) inside Eq. (1), one finds that

$$\sigma_{\text{ff}}(\omega) \approx \frac{4\bar{Z}^2 e^6}{3\sqrt{3}\hbar} \frac{N_i}{(\hbar\omega)^3} \int_0^\infty d\varepsilon [f(\varepsilon) - f(\varepsilon + \hbar\omega)]. \quad (7)$$

The integration in energy leads to

$$\int_0^\infty d\varepsilon [f(\varepsilon) - f(\varepsilon + \hbar\omega)] = \int_0^{\hbar\omega} d\varepsilon f(\varepsilon) = k_B T \log \left(\frac{1 + e^\eta}{1 + e^{\eta - \beta\hbar\omega}} \right), \quad (8)$$

and we obtain

$$\sigma_{\text{ff}}(\omega) \approx \frac{4\bar{Z}^2 e^6}{3\sqrt{3}\hbar} \frac{N_i}{(\hbar\omega)^3} k_B T \log \left(\frac{1 + e^\eta}{1 + e^{\eta - \beta\hbar\omega}} \right). \quad (9)$$

This is the expression found by More [40]. The divergence at low frequencies can be eliminated by inserting a Drude-like factor [10,41],

$$\sigma_{\text{ff}}(\omega) \approx \frac{4\bar{Z}^2 e^6}{3\sqrt{3}\hbar} \frac{N_i}{\gamma^2 + (\hbar\omega)^2} \frac{k_B T}{\hbar\omega} \log \left(\frac{1 + e^\eta}{1 + e^{\eta - \beta\hbar\omega}} \right), \quad (10)$$

where the free parameter γ is tuned such that [10]

$$\int_0^\infty d\omega \sigma_{\text{ff}}(\omega) = \frac{\pi e^2 N_e}{2m_e}, \quad (11)$$

where m_e is the electron mass and $N_e = \bar{Z}N_i$ is the electronic density. Here, we assumed \bar{Z} to be the average ionization of the plasma. Now, if we multiply $\sigma_{\text{ff}}(\omega)$ by $4\pi/c$ in Eq. (10) and make $\gamma = 0$, we obtain the Kramers expression for the free-free photoabsorption coefficient with the degeneracy correction and stimulated emission [35]. With $\gamma \neq 0$, the free-free photoabsorption coefficient reads

$$\alpha_{\text{ff}}(\omega) = \frac{16\pi \bar{Z}^2 e^6}{3\sqrt{3}c\hbar} \frac{N_i}{\gamma^2 + (\hbar\omega)^2} \frac{k_B T}{\hbar\omega} \log \left(\frac{1 + e^\eta}{1 + e^{\eta - \beta\hbar\omega}} \right). \quad (12)$$

It can be shown [41] that stimulated emission is taken into account in this expression.

B. Bound-bound component in the one-electron approximation

Let us now consider the bound-bound component $\sigma_{\text{bb}}(\omega)$ of the real part of the frequency-dependent electrical conductivity [10,34],

$$\sigma_{\text{bb}}(\omega) = \frac{2\pi\omega e^2}{3\Omega} \sum_{\substack{n_i, n_j \\ \ell_i, \ell_j = \ell_i \pm 1}} (f_i - f_j) \ell_{>} \times \left[\int_0^\infty dr P_{n_i \ell_i}(r) r P_{n_j \ell_j}(r) \right]^2 \delta(\varepsilon_j - \varepsilon_i - \hbar\omega), \quad (13)$$

where $f_k = 1/(1 + e^{\beta\varepsilon_k - \eta})$, n_k and ℓ_k are the principal and orbital quantum numbers of orbital k and ε_k its energy. $\sigma_{\text{bb}}(\omega)$

can also be written [42]

$$\begin{aligned} \sigma_{\text{bb}}(\omega) &= \frac{2\pi\omega e^2}{3\Omega} \sum_{\substack{n_i, n_j \\ \ell_i, \ell_j = \ell_i \pm 1 \\ \varepsilon_j > \varepsilon_i}} f_i(1 - f_j)\ell_{>} \\ &\times \left[\int_0^\infty dr P_{n_i\ell_i}(r)r P_{n_j\ell_j}(r) \right]^2 \\ &\times \delta(\varepsilon_j - \varepsilon_i - \hbar\omega)(1 - e^{-\beta\hbar\omega}), \end{aligned} \quad (14)$$

where the one-electron radial parts of the bound wavefunctions $P_{n_i\ell_i}(r)$ are normalized such that [10]

$$\int_0^\infty dr P_{n\ell}(r)P_{n'\ell}(r) = \delta_{nn'}. \quad (15)$$

In Eq. (14), we make apparent the stimulated emission that is included in the Kubo-Greenwood approach [42]. We now introduce the one-electron oscillator-strength [34]

$$\bar{f}_{n_i\ell_i, n_j\ell_j} = \frac{4m_e\omega}{3\hbar} \frac{\ell_{>}}{D_i} (R_{n_i\ell_i}^{n_j\ell_j})^2, \quad (16)$$

where $D_i = 2(2\ell_i + 1)$ is the degeneracy of orbital i and

$$R_{n_i\ell_i}^{n_j\ell_j} = \int_0^\infty dr P_{n_i\ell_i}(r)r P_{n_j\ell_j}(r). \quad (17)$$

We then find that

$$\begin{aligned} \sigma_{\text{bb}}(\omega) &= \frac{he^2}{4m_e\Omega} \sum_{\substack{n_i, n_j \\ \ell_i, \ell_j = \ell_i \pm 1 \\ \varepsilon_j > \varepsilon_i}} D_i f_i(1 - f_j) \bar{f}_{n_i\ell_i, n_j\ell_j} \\ &\times \delta(\varepsilon_j - \varepsilon_i - \hbar\omega)(1 - e^{-\beta\hbar\omega}), \end{aligned} \quad (18)$$

where h is the Planck constant. We now multiply Eq. (18) by $4\pi/c$, and we obtain the expression of the bound-bound photoabsorption coefficient [35] with stimulated emission and a line shape $\varphi_{i \rightarrow j}(\hbar\omega) = \delta(\varepsilon_j - \varepsilon_i - \hbar\omega)$, i.e.,

$$\begin{aligned} \alpha_{\text{bb}}(\omega) &= N_i \frac{\pi h e^2}{m_e c} \sum_{\substack{n_i, n_j \\ \ell_i, \ell_j = \ell_i \pm 1 \\ \varepsilon_j > \varepsilon_i}} D_i f_i(1 - f_j) \bar{f}_{n_i\ell_i, n_j\ell_j} \\ &\times \delta(\varepsilon_j - \varepsilon_i - \hbar\omega)(1 - e^{-\beta\hbar\omega}). \end{aligned} \quad (19)$$

C. Bound-free component in the one-electron approximation

Finally, the bound-free component $\sigma_{\text{bf}}(\omega)$ of the real part of the frequency-dependent electrical conductivity reads [10,34]

$$\begin{aligned} \sigma_{\text{bf}}(\omega) &= \frac{2\pi\omega e^2}{3\Omega} \int_0^\infty d\varepsilon \sum_{\substack{n_i, \ell_i \\ \ell = \ell_i \pm 1}} f_i[1 - f(\varepsilon)]\ell_{>} \\ &\times \left[\int_0^\infty dr P_{n_i\ell_i}(r)r P_{\varepsilon\ell}(r) \right]^2 \\ &\times \delta(\varepsilon - \varepsilon_i - \hbar\omega)(1 - e^{-\beta\hbar\omega}). \end{aligned} \quad (20)$$

Introducing the differential one-electron oscillator strength,

$$\frac{d\bar{f}_{n_i\ell_i, \varepsilon}}{d\hbar\omega} = \frac{4m_e\omega}{3\hbar} \sum_{\ell = \ell_i \pm 1} \frac{\ell_{>}}{D_i} (R_{n_i\ell_i}^{\varepsilon, \ell})^2 \Theta(\hbar\omega + \varepsilon_i), \quad (21)$$

where $\Theta(x)$ is the Heaviside function and

$$R_{n_i\ell_i}^{\varepsilon, \ell} = \int_0^\infty dr P_{n_i\ell_i}(r)r P_{\varepsilon\ell}(r), \quad (22)$$

one obtains

$$\begin{aligned} \sigma_{\text{bf}}(\omega) &= \frac{he^2}{4m_e\Omega} \sum_{\substack{n_i, \ell_i \\ \ell = \ell_i \pm 1}} D_i f_i[1 - f(\varepsilon_i + \hbar\omega)] \\ &\times \frac{d\bar{f}_{n_i\ell_i, \varepsilon_i + \hbar\omega}}{d\hbar\omega} (1 - e^{-\beta\hbar\omega}). \end{aligned} \quad (23)$$

Now, if we multiply Eq. (23) by $4\pi/c$, we find the expression of the bound-free photoabsorption coefficient [35] with stimulated emission, i.e.,

$$\begin{aligned} \alpha_{\text{bf}}(\omega) &= N_i \frac{\pi h e^2}{m_e c} \sum_{\substack{n_i, \ell_i \\ \ell = \ell_i \pm 1}} D_i f_i[1 - f(\varepsilon_i + \hbar\omega)] \\ &\times \frac{d\bar{f}_{n_i\ell_i, \varepsilon_i + \hbar\omega}}{d\hbar\omega} (1 - e^{-\beta\hbar\omega}). \end{aligned} \quad (24)$$

It is common to consider rather the ionization potential $I_i = -\varepsilon_i$ of orbital i .

D. Summary

We have found that for the nonrelativistic average-atom model, the expressions for the photoabsorption coefficients without line profile treatment [35] calculated using the dipole approximation are equivalent to the ones obtained using the Kubo-Greenwood method with an index of refraction equal to one. The Kubo-Greenwood formulas for the real-part of the frequency-dependent electronic electrical conductivity are obtained using the first-order perturbation-theory where the perturbing electric-field is treated classically in the framework of quantum mechanics [10]. The usual expressions for the photoabsorption coefficients [35] are obtained using the first-order perturbation theory in the framework of quantum mechanics where the coupling between the atomic system and the electromagnetic field is treated quantum-mechanically using the dipole approximation [34]. In short, the perturbing field is treated either classically or quantum-mechanically but the result is the same concerning the photoabsorption coefficients with an index of refraction equal to one. Finally, in opacity codes, the bound-bound, bound-free, and free-free photoabsorption coefficients are related to the spectral opacity $\kappa(\omega)$ by the formula

$$\kappa(\omega)\rho = \alpha_{\text{bb}}(\omega) + \alpha_{\text{bf}}(\omega) + \alpha_{\text{ff}}(\omega), \quad (25)$$

where ρ is the mass density.

E. Practical calculation of the index of refraction

We first calculate the bound-bound α_{bb} , bound-free α_{bf} , and free-free α_{ff} photoabsorption coefficients with stimulated emission using opacity codes [35]. We then multiply each component by $c/4\pi$ to obtain the real part of an effective electrical conductivity. If needed, we regularize the free-free component using a Drude-like formula [10]. We deduce the real part of an effective electrical conductivity by adding the three components. From this quantity, we obtain the expression of the index of refraction from the optical coefficients using classical Maxwell equations [8,10,14–16]. We just have to divide the total photoabsorption coefficient from which we started by the index of refraction found that way to obtain a photoabsorption coefficient in dense matter [27,31]. As for emissivity, we have to multiply the usual expression by the index of refraction [27,31], instead of dividing by it as for the total photoabsorption coefficient [27,31]. In the same spirit, the Planck function should be multiplied by the square of the index of refraction [26,27,31,32].

It can be noticed that the present approach becomes questionable when the linear response theory breaks down. Moreover, this method can only be used when the photoabsorption coefficients are evaluated using the dipole approximation. From a theoretical point of view [44], this is challenging to go beyond the present approach, especially including a refined treatment of the ionic structure instead of considering a complete disorder or questioning the line-profile treatment [10,43].

III. NUMERICAL APPLICATIONS

As a first application, we plot on Fig. 1 the electrical conductivity as a function of energy using Eq. (1) with a Drude-like factor (QM) and Eq. (10) (Kramers) for aluminum at 0.1 g/cm^3 and 10 eV using the SCAALP model [46,47]. On this example, we find that the two curves are different. The static electrical conductivity is greater in the QM approach compared to the Kramers approximation, the difference being of the order of a factor two. The Kramers curve is broader

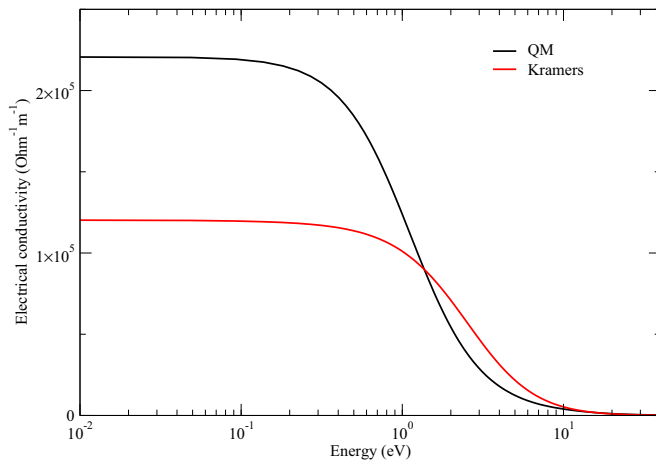


FIG. 1. (Color online) Free-free electrical conductivity as a function of energy for an aluminum plasma at 0.1 g/cm^3 and 10 eV using the SCAALP model. The quantum mechanical (QM) approach is compared to the Kramers (Kramers) approximation.

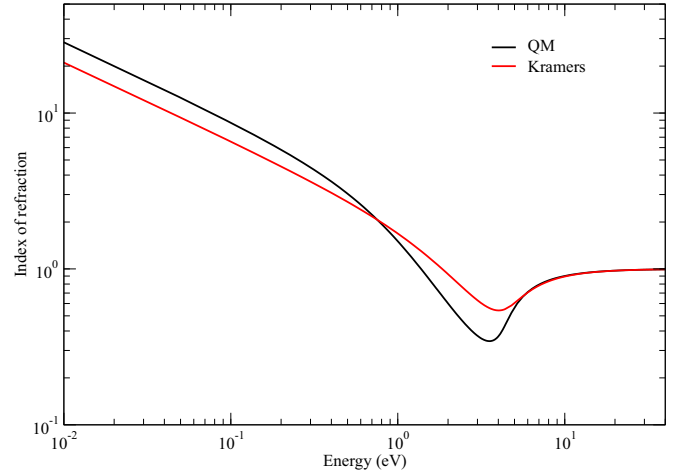


FIG. 2. (Color online) Free-free index of refraction as a function of energy for an aluminum plasma at 0.1 g/cm^3 and 10 eV using the SCAALP model. We use the quantum mechanical (QM) approach and the Kramers (Kramers) approximation to calculate the free-free electrical conductivity.

than the QM curve. This can be understood if we compare the regularization factors. In the first case, we find that $\gamma = 2.7 \text{ eV}$, whereas in the second case, one finds that $\gamma = 1.12 \text{ eV}$. To appreciate the consequences, we plot on Fig. 2 the corresponding indices of refraction using the Kramers-Kronig relations. The two curves present a minimum closed to the plasma frequency equal to 4.40 eV . Finally, we plot on Fig. 3 the spectral opacities. One can see the discrepancy between the two approaches. We deduce that Eq. (10) is an approximation of Eq. (1) with a Drude-like factor, whereas there is no approximation to derive Eq. (18) from Eq. (13) and Eq. (23) from Eq. (20). Using the Kramers approximation instead of a quantum mechanical approach to calculate the free-free electrical conductivity brings about uncertainties, first in the

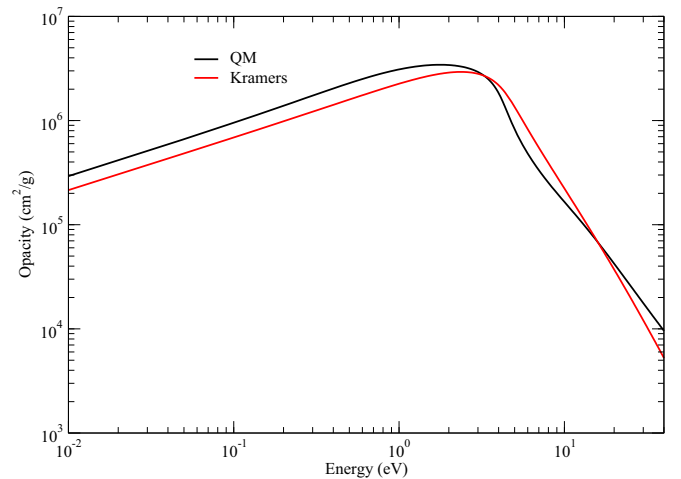


FIG. 3. (Color online) Free-free spectral opacity as a function of energy for an aluminum plasma at 0.1 g/cm^3 and 10 eV using the SCAALP model. We use the quantum mechanical (QM) approach and the Kramers (Kramers) approximation to calculate the free-free electrical conductivity.

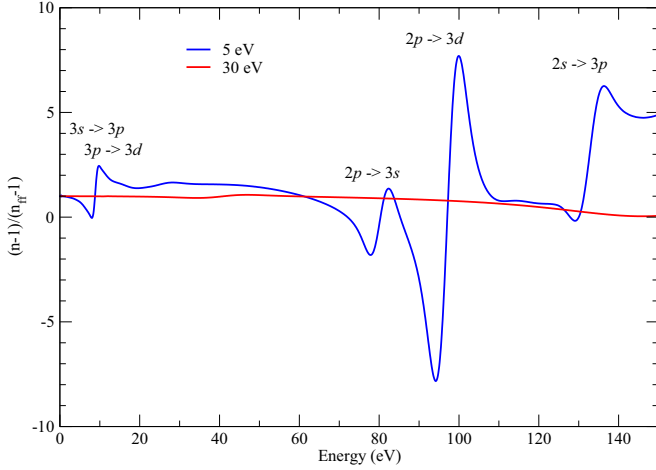


FIG. 4. (Color online) Ratio $(n - 1)/(n_{\text{ff}} - 1)$ as a function of energy for an aluminum plasma at 5 and 30 eV using the SHAAM model.

electrical conductivity, second in the index of refraction, and then in the spectral opacity when we multiply by $4\pi/c$ the electrical conductivity and divide the result by the index of refraction. It is clear that we should rather use the quantum mechanical approach. But it is not always possible in practice for computation time and numerical reasons. The Kramers approximation is a reasonable approximation to calculate the free-free component.

Second, we have implemented the method of calculation of the index of refraction in the opacity code OPAS [45] used as a post-processor of the average-atom model SCAALP [46,47]. We have also implemented this approach in the SHAAM model [48–51]. As an illustration, let us consider the aluminum cases considered by Johnson *et al.* [10]. These authors did calculations for a LTE aluminum plasma at ion density 10^{20} cm^{-3} for temperatures varying between 1 and 30 eV using an average-atom model without statistical broadening of the bound-bound and bound-free transitions. Here, we consider the SHAAM model, which is a screened-hydrogenic average-atom model with statistical treatments of the radiative transitions, and the OPAS code that combines detailed configuration and line accounting treatments. We consider the ratio $(n - 1)/(n_{\text{ff}} - 1)$, where n is the index of refraction including bound-bound, bound-free, and free-free transitions and n_{ff} the index of refraction that includes only free-free transitions. This ratio is very useful to see the impact of the bound subshells on the refractive index. In Fig. 4, we plot the ratio for 5 and 30 eV using the SHAAM code. We can see the impact of the bound subshells on the ratio. At 5 eV, there are many structures. There is a group of two structures merged into one at low energy corresponding to transitions $3s \rightarrow 3p$ and $3p \rightarrow 3d$. We can see at higher energy the presence of transitions $2p \rightarrow 3s$, $2p \rightarrow 3d$, and $2s \rightarrow 3p$. The features are broad due to the statistical treatment. At 30 eV, these features have disappeared and the ratio is close to one. Indeed, we can see a small structure around 40 eV due to the transition $2s \rightarrow 2p$. The structures corresponding to the transitions $2p \rightarrow 3s$, $2p \rightarrow 3d$, and $2s \rightarrow 3p$ become broader due to the statistical fluctuations and move to higher energies. The discrepancy with respect

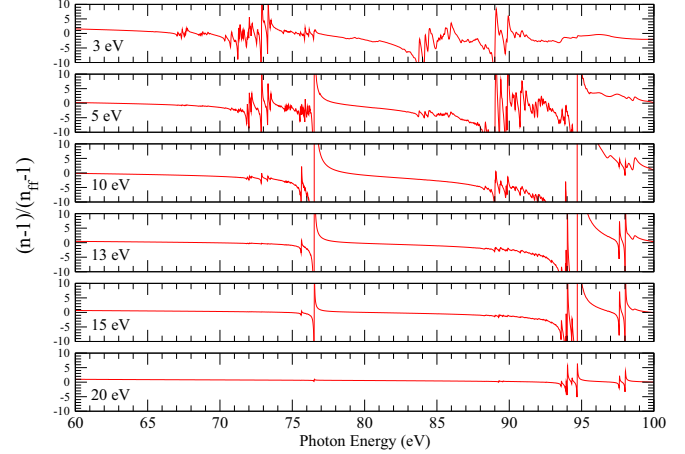


FIG. 5. (Color online) Ratio $(n - 1)/(n_{\text{ff}} - 1)$ as a function of energy for an aluminum plasma between 3 and 20 eV using the OPAS code in DLA treatment.

to one is due to the transitions $2p \rightarrow 3s$ and $2p \rightarrow 3d$. The refractive index is greater than one in the vicinity of 8 eV, 78 eV, 94 eV, and 129 eV, which correspond to the local minimum of the various features. In these circumstances, the observed fringe lines bend in the opposite direction than expected if the index of refraction is simply given by free electrons [2]. To go deeper, OPAS calculations are shown on Fig. 5 for various temperatures between 3 and 20 eV. Using a detailed line accounting (DLA) treatment, we are able to identify most of the ionic stage contributions. For example, the resonant structures around 76 eV (94 eV) are $2p - 3s$ ($2p - 3d$) transitions from the neon-like ground configuration. Because of its closed-shell atomic structure, Ne-like ground configuration is present in an extended range of temperatures. According to the average ionization variation with respect to the temperature, the contribution of this ionic stage is more and more visible for temperatures up to 10 eV. For higher temperatures, the Ne-like ionic fraction progressively decreases, its spectral appears to be weaker and weaker. For a photon energy equals 84.4 eV (corresponding to the 14.7 nm Ni-like Pd soft X-ray laser), the ratio $(n - 1)/(n_{\text{ff}} - 1)$ we calculate is always negative for temperature up to 15 eV. It varies between -3.76 for $T = 3 \text{ eV}$ and -0.41 for $T = 15 \text{ eV}$. For the highest temperature, this ratio is positive and equal to 0.44. Such ratio values are compatible with those obtained using the effective scattering factors given in Ref. [1].

IV. CONCLUSION

In this paper, we proposed a simple method to calculate the index of refraction from existing opacity codes in warm and hot dense matter. This method is sounded as long as the spectral opacity is calculated using the dipole approximation. It is based on the calculation of an effective electrical conductivity derived from the spectral opacity without index of refraction. The index of refraction is thus calculated using this effective electrical conductivity. The spectral opacity with index of refraction is then obtained by dividing the spectral opacity without index of refraction we start from by the index of refraction obtained by our method. The calculated

bound-bound, bound-free, and free-free photoabsorption coefficients from opacity codes are valid down to a few eV's in the plasma regime, so inside the warm dense matter regime. Doing so, this approach can be useful to analyze experimental results involving the refractive index in warm and hot dense matter.

ACKNOWLEDGMENTS

We are indebted to Walter Johnson for helpful comments and remarks concerning the Kubo-Greenwood approach in the framework of the average-atom model. We thank P. Combis for the Kramers-Kronig subroutine.

-
- [1] J. Filevich, J. Grava, M. Purvis, M. C. Marconi, J. J. Rocca, J. Nilsen, J. Dunn, and W. R. Johnson, *Phys. Rev. E* **74**, 016404 (2006).
- [2] J. Nilsen, J. I. Castor, C. A. Iglesias, K. T. Cheng, J. Dunn, W. R. Johnson, J. Filevich, M. A. Purvis, J. Grava, and J. J. Rocca, *High Energy Density Phys.* **4**, 107 (2008).
- [3] G. O. Williams, H.-K. Chung, S. M. Vinko, S. Künzel, A. B. Sardinha, Ph. Zeitoun, and M. Fajardo, *Phys. Plasmas* **20**, 042701 (2013), and references therein.
- [4] R. Kubo, *J. Phys. Soc. Jpn.* **12**, 570 (1957).
- [5] D. A. Greenwood, *Proc. Phys. Soc. London* **71**, 585 (1958).
- [6] M. P. Desjarlais, J. D. Kress, and L. A. Collins, *Phys. Rev. E* **66**, 025401 (2002).
- [7] S. Mazevet, L. A. Collins, N. H. Magee, J. D. Kress, and J. J. Keady, *Astron. Astrophys.* **405**, L5 (2003).
- [8] S. Mazevet, M. P. Desjarlais, L. A. Collins, J. D. Kress, and N. H. Magee, *Phys. Rev. E* **71**, 016409 (2005).
- [9] S. Mazevet, M. Torrent, V. Recoules, and F. Jollet, *High Energy Density Phys.* **6**, 84 (2010).
- [10] W. R. Johnson, C. Guet, and G. F. Bertsch, *J. Quant. Spectrosc. Radiat. Transf.* **99**, 327 (2006).
- [11] M. Yu. Kuchiev and W. R. Johnson, *Phys. Rev. E* **78**, 026401 (2008).
- [12] W. R. Johnson, *High Energy Density Phys.* **5**, 61 (2009).
- [13] C. E. Starrett, J. Clérouin, V. Recoules, J. D. Kress, L. A. Collins, and D. E. Hanson, *Phys. Plasmas* **19**, 102709 (2012).
- [14] J. M. Ziman, *Principles of the Theory of Solids* (Cambridge University Press, Cambridge, 1979).
- [15] W. Jones and N. H. March, *Theoretical Solid States Physics*, Vols. 1 and 2 (Dover, New York, 1985).
- [16] G. R. Fowles, *Introduction to Modern Optics* (Dover, New York, 1989).
- [17] S. M. Vinko, G. Gregori, M. P. Desjarlais, B. Nagler, T. J. Whitcher, R. W. Lee, P. Audebert, and J. S. Wark, *High Energy Density Phys.* **5**, 124 (2009).
- [18] C. A. Iglesias, *High Energy Density Phys.* **6**, 311 (2010).
- [19] C. A. Iglesias, *High Energy Density Phys.* **7**, 38 (2011).
- [20] S. M. Vinko, G. Gregori, and J. S. Wark, *High Energy Density Phys.* **7**, 40 (2011).
- [21] R. Benattar, C. Galos, and P. Ney, *J. Quant. Spectrosc. Radiat. Transf.* **54**, 53 (1995).
- [22] J. Nilsen, W. R. Johnson, C. A. Iglesias, and J. H. Scofield, *J. Quant. Spectrosc. Radiat. Transf.* **99**, 425 (2006).
- [23] L. A. Wilson and G. J. Tallents, *High Energy Density Phys.* **9**, 402 (2013).
- [24] L. M. R. Gartside, G. J. Tallents, A. K. Rossall, E. Wagenaars, D. S. Whittaker, M. Kozlová, J. Nejd, M. Sawicka, J. Polan, M. Kalal, and B. Rus, *Optics Lett.* **35**, 3820 (2010).
- [25] L. M. R. Gartside, G. J. Tallents, A. K. Rossall, E. Wagenaars, D. S. Whittaker, M. Kozlová, J. Nejd, M. Sawicka, J. Polan, M. Kalal, and B. Rus, *High Energy Density Phys.* **7**, 91 (2011).
- [26] G. Bekefi, *Radiation Processes in Plasmas* (Wiley, New York, 1966).
- [27] J. P. Cox and R. T. Giuly, *Principles of Stellar Structure*, Vols. 1 and 2 (Gordon and Breach, New York, 1968).
- [28] F. Perrot, *Laser Part. Beams* **14**, 731 (1996).
- [29] B. J. B. Crowley and J. W. Harris, *J. Quant. Spectrosc. Radiat. Transf.* **71**, 257 (2001).
- [30] C. A. Iglesias, F. J. Rogers, and D. Saumon, *Astrophys. J.* **569**, L111 (2002).
- [31] J. I. Castor, *Radiation Hydrodynamics* (Cambridge University Press, Cambridge, 2007).
- [32] J. R. Howell, R. Siegel, and M. Pinar Mengüç, *Thermal Radiation Heat Transfer* (Taylor & Francis Group, New York, 2011).
- [33] R. P. Feynman, R. B. Leighton, and M. Sands, *The Feynman Lectures on Physics* (Basic Books, New York, 2011).
- [34] I. I. Sobelman, *Atomic Spectra and Radiative Transitions*, 2nd ed. (Springer-Verlag, Berlin, 1992).
- [35] S. Rose, *Laser Plasma Interactions 5: Inertial Confinement Fusion* (IOP, London, 1995).
- [36] G. Peach, *Mon. Not. R. Astron. Soc.* **130**, 361 (1965).
- [37] R. T. Johnston, *J. Quant. Spectrosc. Radiat. Transf.* **7**, 815 (1967).
- [38] B. F. Rozsnyai and M. Lamoureux, *J. Quant. Spectrosc. Radiat. Transf.* **43**, 381 (1990).
- [39] B. Wilson, C. Iglesias, and M. Chen, *J. Quant. Spectrosc. Radiat. Transf.* **81**, 499 (2003).
- [40] R. M. More, *J. Plasma Fusion Res.* **76**, 623 (2000).
- [41] G. Faussurier, C. Blancard, P. Combis, and L. Videau, *Phys. Plasmas* **21**, 092706 (2014).
- [42] W. A. Harrison, *Solid State Physics* (Dover, New York, 1979).
- [43] I. I. Sobel'man, L. A. Vainshtein, and E. A. Yukov, *Excitation of Atoms and Broadening of Spectral Lines*, 2nd ed. (Springer-Verlag, Berlin, 1995).
- [44] C. Fortmann, Ph.D. Thesis, Rostock University, Rostock, Germany, 2008.
- [45] C. Blancard, P. Cossé, and G. Faussurier, *Astrophys. J.* **745**, 10 (2012).
- [46] C. Blancard and G. Faussurier, *Phys. Rev. E* **69**, 016409 (2004).
- [47] G. Faussurier, C. Blancard, P. Cossé, and P. Renaudin, *Phys. Plasmas* **17**, 052707 (2010).
- [48] G. Faussurier, C. Blancard, and A. Decoster, *Phys. Rev. E* **56**, 3474 (1997).
- [49] G. Faussurier, C. Blancard, and A. Decoster, *Phys. Rev. E* **56**, 3488 (1997).
- [50] G. Faussurier, C. Blancard, and E. Berthier, *Phys. Rev. E* **63**, 026401 (2001).
- [51] P. Morel, V. Méot, G. Gosselin, G. Faussurier, and C. Blancard, *Phys. Rev. C* **81**, 034609 (2010).